

Abundant Z-cyanomethanimine in the interstellar medium: paving the way to the synthesis of adenine

V. M. Rivilla^{1*}, J. Martín-Pintado², I. Jiménez-Serra², S. Zeng³, S. Martín^{4,5}, J. Armijos-Abendaño⁶, M. A. Requena-Torres⁷, R. Aladro⁸, and D. Riquelme⁸

¹INAF-Osservatorio Astrofisico di Arcetri, Largo Enrico Fermi 5, I-50125, Florence, Italy

²Centro de Astrobiología (CSIC-INTA). Ctra de Ajalvir, km. 4, Torrejón de Ardoz, 28850 Madrid, Spain

³School of Physics and Astronomy, Queen Mary University of London, Mile End Road, E1 4NS London, United Kingdom

⁴European Southern Observatory (ESO), Alonso de Córdova 3107, Vitacura, Santiago, Chile

⁵Joint ALMA Observatory, Alonso de Córdova 3107, Vitacura, Santiago, Chile

⁶Observatorio Astronómico de Quito, Escuela Politécnica Nacional, Av. Gran Colombia S/N, Interior del Parque La Alameda, 170136, Quito, Ecuador

⁷University of Maryland, College Park, ND 20742-2421

⁸Max-Planck-Institut für Radioastronomie, Auf dem Hügel 69, 53121 Bonn,

Accepted XXX. Received YYY; in original form ZZZ

ABSTRACT

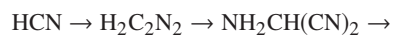
We report the first detection in the interstellar medium of the Z-isomer of cyanomethanimine (HNCHCN), an HCN dimer proposed as precursor of adenine. We identified six transitions of Z-cyanomethanimine, along with five transitions of E-cyanomethanimine, using IRAM 30m observations towards the Galactic Center quiescent molecular cloud G+0.693. The Z-isomer has a column density of $(2.0 \pm 0.6) \times 10^{14} \text{ cm}^{-2}$ and an abundance of 1.5×10^{-9} . The relative abundance ratio between the isomers is $[Z/E] \sim 6$. This value cannot be explained by the two chemical formation routes previously proposed (gas-phase and grain surface), which predicts abundances ratios between 0.9 and 1.5. The observed $[Z/E]$ ratio is in good agreement with thermodynamic equilibrium at the gas kinetic temperature (130–210 K). Since isomerization is not possible in the ISM, the two species may be formed at high temperature. New chemical models, including surface chemistry on dust grains and gas-phase reactions, should be explored to explain our findings. Whatever the formation mechanism, the high abundance of Z-HNCHCN shows that precursors of adenine are efficiently formed in the ISM.

Key words: Galaxy: centre – ISM: molecules – ISM: abundances – ISM: clouds

1 INTRODUCTION

Understanding the origin of life on Earth is one of the most challenging problems in astrophysics in the framework of astrobiology. To shed light on this complex topic, it is absolutely needed a comprehensive study of the chemical complexity of the interstellar medium (ISM) that feeds the formation of stars and planets. In this sense, the chemical family of nitriles can give important clues. Nitriles, organic compounds with a $\text{C}\equiv\text{N}$ functional group, play a crucial role in prebiotic chemistry since they are key intermediates in the formation of amino acids, peptides, nucleic acids and nucleobases (e.g. Balucani 2009). Adenine ($\text{H}_5\text{C}_5\text{N}_5$), one of the nucleobases of DNA and RNA, is a basic ingredient in the RNA-world scenario for the origin of life

on Earth (e.g. Kaiser & Balucani 2001, Ehrenfreund et al. 2001, Bernstein et al. 2004). Oró (1961) reported the synthesis of adenine from a solution of HCN and NH_3 under conditions similar to those thought to have existed on the primitive Earth. Chakrabarti & Chakrabarti (2000) proposed that adenine might be formed during the chemical evolution of a star-forming molecular cloud through the oligomerization of HCN in the gas phase in four steps:



However, by performing theoretical calculations, Smith et al. (2001) and Yim & Choe (2012) showed that the first step, i.e. the formation of an HCN dimer from two HCN molecules, does not occur efficiently in the conditions of the

* E-mail: rivilla@arcetri.astro.it

ISM. Therefore, the question of how HCN dimers can be formed remains open. Since they are precursors of adenine, understanding their formation mechanisms is of crucial importance from an astrobiological point of view.

The most stable dimer of HCN is C-cyanomethanimine (HNCHCN hereafter), which presents two different isomers: the Z-isomer and the E-isomer (Clemmons et al. 1983). These species are stereoisomers about the double bond $N=C$ (see e.g. Fig. 1 of Takano et al. 1990) and the conversion from the Z- to the E-isomer requires an energy of 15.95 kK. The laboratory experiments and chemical calculations by Takano et al. (1990) and Zaleski et al. (2013), respectively, indicate that the Z-isomer is more stable and lower in energy than the E-isomer, with an estimated energy difference in the range 238–382 K. Nevertheless, only the high-energy E-isomer has been detected in the ISM so far. Several lines were reported in absorption towards the bright continuum of the cluster of hot cores located in the SgrB2N complex (Zaleski et al. 2013), while the Z-conformer was elusive. Recent searches of the Z-conformer in a sample of low-mass star-forming regions have also been unsuccessful (Melosso et al. 2018).

In this work, we report the results of an interstellar search for the Z-conformer of HNCHCN (Z-HNCHCN hereafter). Using an IRAM 30m spectral survey, we searched for this species in the G+0.693-0.027 giant molecular cloud (G+0.693 hereafter) in the Galactic Center. This region exhibits high gas kinetic temperatures ranging from ~ 50 K to ~ 150 K (Guesten et al. 1985; Hüttelmeister et al. 1993; Rodríguez-Fernández et al. 2001; Ginsburg et al. 2016; Krieger et al. 2017; Zeng et al. 2018), low dust temperatures of ≤ 30 K (Rodríguez-Fernández et al. 2004), and relatively low H_2 gas densities ($\sim 10^4$ cm $^{-3}$; Rodríguez-Fernández et al. 2000). Due to the low H_2 densities, the molecules are sub-thermally excited and hence the excitation temperatures are low (~ 5 –20 K; Requena-Torres et al. 2006; Martín et al. 2008; Rivilla et al. 2018; Zeng et al. 2018). G+0.693 is one of the most chemically rich reservoirs in our Galaxy. Many molecular species have been identified in this cloud, including some of prebiotic relevance such as complex organic molecules (COMs; Requena-Torres et al. 2006, 2008; Zeng et al. 2018) and phosphorus-bearing species (Rivilla et al. 2018). In particular, numerous nitrile molecules have been already detected in the source such as C_3N , HC_3N , HC_5N , HC_7N , CH_2CN , CH_3CN , CH_3C_3N , NH_2CN and $HOCN$ (Zeng et al. 2018). This rich nitrile chemistry makes this source an excellent target to search for more complex nitriles, and in particular Z-HNCHCN.

2 OBSERVATIONS

We used in this work a spectral line survey towards the quiescent molecular cloud G+0.693 carried out with the IRAM

Table 1. Transitions of HNCHCN detected towards G+0.693.

Frequency (GHz)	Transition	$\log A_{ul}$ (s $^{-1}$)	E_{up} (K)	$\int T_A^* dv$ (K km s $^{-1}$)	Detection level
Z-isomer					
85.283	9(1,9)–8(1,8)	-5.2107	23	0.68 \pm 0.25	13.8
86.996	9(0,9)–8(0,8)	-5.1795	21	0.91 \pm 0.30	15.9
89.247	9(1,8)–8(1,7)	-5.1515	24	0.63 \pm 0.24	7.7
94.735	10(1,10)–9(1,9)	-5.0705	27	0.47 \pm 0.21	13.7
96.569	10(0,10)–9(0,9)	-5.0413	26	0.62 \pm 0.25	7.1
109.017	11(1,10)–10(1,9)	-4.8849	34	0.27 \pm 0.16	4.8
E-isomer					
84.425	9(1,9)–8(1,8)	-4.4608	23	0.71 \pm 0.05	13.9
93.791	10(1,10)–9(1,9)	-4.3204	28	0.51 \pm 0.04	11.3
95.422	10(0,10)–9(0,9)	-4.2937	25	0.71 \pm 0.05	17.9
97.501	10(1,9)–9(1,8)	-4.2698	29	0.47 \pm 0.04	8.4
104.895	11(0,11)–10(0,10)	-4.1684	30	0.46 \pm 0.03	6.9

30m telescope at Pico Veleta¹ (Spain) and the NRAO² 100 m Robert C. Byrd Green Bank telescope (GBT) in West Virginia (USA), covering frequencies from 12 to 272 GHz. The observations were centered at the coordinates $\alpha(J2000.0)=17^h 47^m 22^s$ and $\delta(J2000.0)=-28^\circ 21' 27''$. We refer to Zeng et al. (2018) for more detailed information on the observations.

3 ANALYSIS AND RESULTS

The identification of the lines was performed using the SLIM (Spectral Line Identification and Modeling) tool of the MADCUBA package³, which contains the spectroscopic information from the Cologne Database for Molecular Spectroscopy (CDMS⁴) (Müller et al. 2001, 2005; Endres et al. 2016) and the Jet Propulsion Laboratory (JPL) catalogue⁵ (Pickett et al. 1998). We have used the CDMS entries for the two isomers of HNCHCN, which contain the spectroscopy from Takano et al. (1990), Zaleski et al. (2013) and Melosso et al. (2018). Since there are not collisional coefficients available for these species we performed the analysis assuming local thermodynamic equilibrium conditions (LTE). We generated with SLIM-MADCUBA a synthetic spectrum to compare with the observations. We confirmed the presence of ten transitions of Z-HNCHCN in the spectra towards G+0.693 with a significant detection level ($>4\sigma$; see below). Six of these transitions are unblended, i.e., they are not contaminated by emission from other molecular

¹ This paper makes use of observations obtained with the IRAM-30m telescope. IRAM is supported by INSU/CNRS (France), MPG (Germany), and IGN (Spain).

² The National Radio Astronomy Observatories is a facility of the National Science Foundation, operated under a cooperative agreement by Associated Universities, Inc.

³ Madrid Data Cube Analysis on ImageJ is a software developed at the Center of Astrobiology (CAB) in Madrid; <http://cab.inta-csic.es/madcuba/Portada.html>; see Martín et al., in prep; Rivilla et al. (2016, 2017a).

⁴ <http://www.astro.uni-koeln.de/cdms>

⁵ <http://spec.jpl.nasa.gov/>

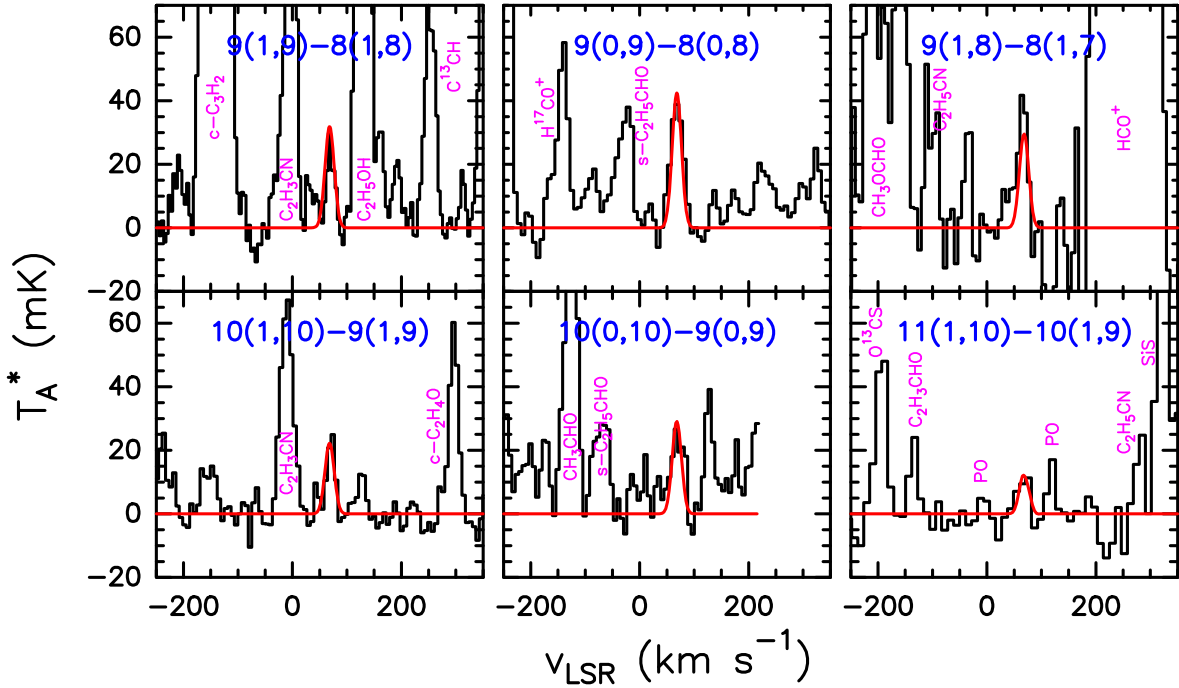


Figure 1. IRAM 30m spectra of Z-HNCHCN towards the Galactic Center quiescent giant molecular cloud G+0.693. The red curves correspond to the LTE best fit obtained with MADCUBA-AUTOFIT. The quantum numbers of each transition are shown in blue in each panel (see also Table 1). Other molecular species identified in the spectra are indicated with magenta labels.

species, while the other four are blended with other species. We checked that the unblended transitions are not associated with any of the >90 species we have identified toward this source (Requena-Torres et al. 2008; Rivilla et al. 2018; Zeng et al. 2018; see Figure 1). We note that not a single transition of Z-HNCHCN predicted by the LTE spectrum is missing in the data. The spectroscopic information of the six unblended transitions are summarized in Table 1, and the spectra are shown in Figure 1. This is the first detection of this species in the ISM.

Then, we used the MADCUBA-AUTOFIT tool that compares the observed spectra with the LTE synthetic spectra, taking into account all the transitions considered, and it provides the best non-linear least-squared fit using the Levenberg-Marquardt algorithm. The free parameters in the fit are: column density (N) of the molecule, excitation temperature (T_{ex}), velocity (v), and full width half maximum ($FWHM$). We did not apply a beam dilution factor since it is well known that the molecular emission towards this source is extended over the beam (e.g. Requena-Torres et al. 2006; Martín et al. 2008; Rivilla et al. 2018). For Z-HNCHCN, since the algorithm did not converge leaving all four parameters free, we fixed the linewidth to 20 km s^{-1} , which reproduces well the observed spectra and it is consistent with the values inferred for other -CN species (Zeng et al. 2018), and rerun AUTOFIT. The results of the fit are summarized in Table 2. We derived an excitation temperature of $8 \pm 2 \text{ K}$, very similar to that determined for other complex species in this region (Requena-Torres et al. 2008; Zeng et al. 2018), and a column density of $(2.0 \pm 0.6) \times 10^{14} \text{ cm}^{-2}$. We present in Table 1 the velocity integrated intensity ($\int T_A^* dv$) of the identified transitions resulting from the fit. We calculated the detection level of each transition comparing the velocity

integrated intensity with $rms \times \sqrt{\delta v / FWHM} \times FWHM$, where rms is the noise measured in line-free spectral ranges close to each transition, and δv is the spectral resolution of the spectra. Three of the identified transitions of Z-HNCHCN are above 13σ , two above 7σ and one above 4σ (Table 1).

We repeated the analysis for the E-isomer. We identified eight transitions above $>4\sigma$, of which five are unblended (Table 1 and Figure 2). Since the AUTOFIT algorithm did not converge leaving T_{ex} as a free parameter, we fixed it to the value found for the Z-isomer, 8 K. We obtained a column density of $(0.33 \pm 0.03) \times 10^{14} \text{ cm}^{-2}$. Three transitions are detected above 11σ , and two above 6σ (Table 1). Both conformers have velocities of around $\sim 68 \text{ km s}^{-1}$, consistently with many other molecules observed towards this region (see e.g. Zeng et al. 2018). The molecular ratio between the two conformers is $[Z/E] = 6.1 \pm 2.4$. The total molecular abundance of C-cyanomethanimine, considering both isomers, is 1.74×10^{-9} .

We derived the fractional molecular abundances by dividing their column densities by the H_2 column density (N_{H_2}) measured in G+0.693. We adopted $N_{\text{H}_2} = 1.35 \times 10^{23} \text{ cm}^{-2}$ as inferred by Martín et al. (2008) from C^{18}O observations. In our calculations, we assumed that all molecules show a similar spatial distribution than C^{18}O , i.e. all molecules arise from the same volume. The derived abundances are presented in Table 2. The Z-isomer has a relatively high abundance of 1.5×10^{-9} , which is comparable to those of other nitrogen-bearing species in this source such as CH_3CN or HC_5N and higher than those of e.g. CH_3NCO and $\text{C}_2\text{H}_5\text{CN}$ (Zeng et al. 2018).

We also searched in the spectra of G+0.693 for other molecules that have been proposed as possible precursors of HNCHCN (see further discussion in Section 4):

the cyanogen radical (CN), methanimine (CH₂NH) and cyanogen (NCCN). Since CN is optically thick towards G+0.693, we have analyzed the optically thin isotopologue ¹³CN. The spectra and the spectroscopic information of the studied ¹³CN transitions are shown in Appendix A. The results of AUTOFIT are presented in Table 2. Assuming the isotopic ratio of ¹²C/¹³C~21 derived in this source by Armijos-Abendaño et al. (2014), we obtained a CN fractional abundance of 1.5×10⁻⁸. The results of CH₂NH were previously presented in Zeng et al. (2018) and are also shown in Table 2.

Since the detection of NCCN is not possible through radio and millimeter observations due to the lack of a permanent electric dipole moment, we searched for its protonated form, NCCNH⁺. We confirmed the presence of this species through the detection of the J=10-9 and J=11-10 rotational transitions (see Appendix A). To our knowledge this is the third detection of this species in the ISM after those in the dark cloud TMC-1 and the L483 dense core (Agúndez et al. 2015). Our analysis yielded a fractional molecular abundance of 1.4×10⁻¹² for this species (Table 2). If we assume a [NCCNH⁺]/[NCCN] ratio of ~10⁻⁴ as inferred from the chemical modelling of Agúndez et al. (2015), the abundance of NCCN would be 1.4×10⁻⁸ cm⁻².

4 DISCUSSION

Due to the lack of detections, very little is known about the formation of HNCHCN. There is no chemical formation route of this species included in the astrochemical databases KIDA⁶ (Wakelam et al. 2012) and UMIST⁷ (McElroy et al. 2013). Zaleski et al. (2013) suggested that radical chemistry on the surface of dust grains might form HNCHCN. More recently, two possible formation routes have been proposed. Vazart et al. (2015) studied the neutral-neutral gas-phase reaction between the cyanogen radical and methanimine:



A different chemical pathway has been proposed by Shivani et al. (2017) both on the surface of icy dust grains and in the gas phase:



All proposed formation paths seem to be barrierless, which suggests that both gas-phase and grain surface reactions are able to form efficiently HNCHCN provided that the precursors are sufficiently abundant. Our data indicate that the reactants of the proposed reactions (CN, CH₂NH and NCCN) are relatively abundant in G+0.693, with abundances ranging from 4×10⁻⁹ to 1.5 ×10⁻⁸ (Table 2), which are higher than the derived abundance of HNCHCN by factor of around 9, 2 and 8, respectively. This suggests that these mechanisms might be able to explain the high abundance of HNCHCN (1.74×10⁻⁹) inferred in this cloud.

Since we have detected for the first time both isomers,

we can use the [Z/E] ratio to constrain the proposed formation scenarios. Vazart et al. (2015) showed that the gas-phase formation route from CN and CH₂NH produces a ratio [Z/E]~1.5, regardless of the temperature. The calculations by Shivani et al. (2017) predict a [Z/E] ratio of 0.9 in gas-phase and of 1 on the surface of dust grains. Therefore, both pathways fail to explain the observed ratio of ~6, which might indicate that we are missing key formation routes and/or destruction reactions. A complete study including all the formation and destruction channels of the involved species is needed before drawing firm conclusions.

Interestingly, the [Z/E] ratio found in G+0.693 seems to indicate that the two isomers are close to thermodynamic equilibrium at the kinetic temperature T_k of the cloud. If this is the case, the abundances of the isomers are related through the expression:

$$[Z/E] = \frac{N(Z)}{N(E)} = \frac{1}{g} \times \exp\left(\frac{\Delta E}{T_k}\right), \quad (3)$$

where ΔE is the energy difference between the isomers, and g accounts for the statistical weights, which in this case is 1. Takano et al. (1990) derived experimentally an energy difference of 237–382 K, which is in good agreement with the value of 370 K inferred with the quantum chemical calculations by Zaleski et al. (2013), and with the value of 307 K more recently estimated by Puzzarini (2015). Then, the observed [Z/E] ratio of 6.1 implies a T_k in the range 130–210 K, which is in good agreement with the kinetic temperature found by Zeng et al. (2018) in G+0.693. This suggests that the two isomers are in thermodynamic equilibrium at the T_k of the gas. We note that also the populations of other isomers in the ISM seem to be in thermodynamic equilibrium at T_k , as e.g. the conformers of ethyl formate (C₂H₅OCHO) in the hot molecular cores located in the W51 and Orion KL regions (Rivilla et al. 2017b; Tercero et al. 2013). Since the isomerization barrier between the E- and Z-isomers of HNCHCN is very high (15.95 kK; Zaleski et al. 2013) this process cannot occur in the ISM. This means that the T_k derived from eq. 3 reflects the temperature at which the molecules were formed. Since the dust in G+0.693 is cold (≤ 30 K; Rodríguez-Fernández et al. 2004), and the gas temperatures are high (~50 K to ~150 K; e.g. Guesten et al. 1985; Hüttelmeister et al. 1993; Rodríguez-Fernández et al. 2001; Ginsburg et al. 2016; Krieger et al. 2017; Zeng et al. 2018), this opens two possible chemical pathways:

i) gas-phase reactions occurring at the high kinetic temperatures of the cloud; and

ii) formation on dust triggered by non-thermal energetic events like cosmic-ray impacts, and their subsequent release by grain sputtering in moderate-velocity shock waves. The latter scenario is plausible in the case of G+0.693 since large-scale low-velocity shocks are widespread in the region due to the encounter of two streams of molecular gas (Hasegawa et al. 1994; Henshaw et al. 2016). However, the current observations do not allow to discriminate between these two possible chemical routes.

Whatever the formation mechanism, our analysis of the first detection in the ISM of the Z-isomer of HNCHCN reveals that its abundance is higher than that of the E-conformer by a factor of 6. Given the proposed role of HNCHCN as precursor of adenine (Eschenmoser

⁶ Kinetic Database for Astrochemistry: <http://kida.obs.u-bordeaux1.fr>

⁷ <http://udfa.ajmarkwick.net/index.php>

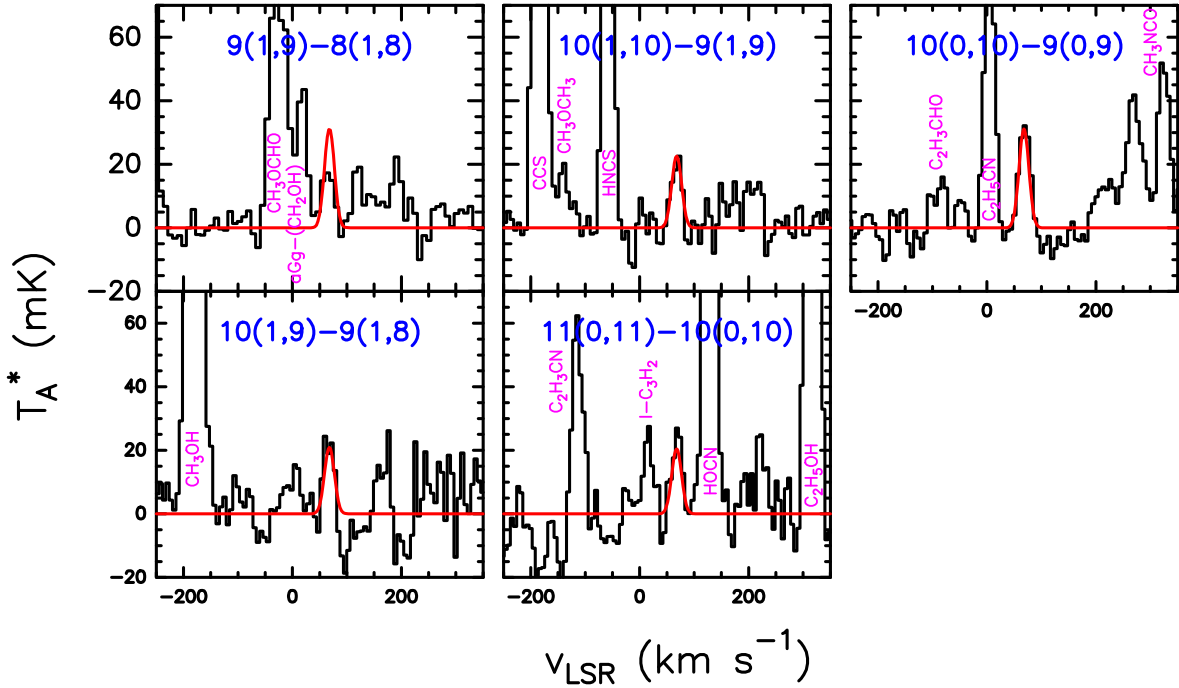


Figure 2. IRAM 30m spectra of E-HNCHCN towards the Galactic Center quiescent giant molecular cloud G+0.693. The red curves correspond to the LTE best fit obtained with MADCUBA-AUTOFIT. The quantum numbers of each transition are shown in blue in each panel (see also Table 1). Other molecular species identified in the spectra are indicated with magenta labels.

Table 2. Derived parameters of the HNCHCN isomers detected towards G+0.693

Species	N ($\times 10^{14} \text{ cm}^{-2}$)	T_{ex} (K)	v_{LSR} (km s^{-1})	FWHM (km s^{-1})	Abundance ($\times 10^{-10}$)
Z-HNCHCN	2.0 ± 0.6	8 ± 2	68.3 ± 0.8	$20^{(a)}$	15
E-HNCHCN	0.33 ± 0.03	$8^{(a)}$	68.0 ± 0.8	21 ± 2	2.4
^{13}CN	0.94 ± 0.03	$10^{(a)}$	71.6 ± 0.4	18.8 ± 0.9	7.0
CN					$150^{(c)}$
$\text{CH}_2\text{NH}^{(b)}$	5.4 ± 0.3	9.7 ± 0.4	69 ± 1	25 ± 1	40
NCCNH^+	0.0019 ± 0.004	$10^{(a)}$	69 ± 2	22 ± 5	0.014
NCCN					$140^{(d)}$

(a) Parameter fixed in the MADCUBA-AUTOFIT analysis. (b) From Zeng et al. (2018). (c) Assuming the isotopic ratio of $^{12}\text{C}/^{13}\text{C} \sim 21$ derived in G+0.693 by Armijos-Abendaño et al. (2014). (d) Assuming a $[\text{NCCNH}^+]/[\text{NCCN}]$ ratio of $\sim 10^{-4}$, as inferred from chemical modelling by Agúndez et al. (2015).

2007; Chakrabarti & Chakrabarti 2000; Balucani 2012; Jung & Choe 2013), the relative high abundance of this species, 1.5×10^{-9} , argues in favor of an efficient synthesis of key precursors of adenine in space. This is a crucial step to understand how the basic ingredients of life could have been assembled in the ISM before their incorporation to the primitive Earth. The role of HNCHCN in the formation of more complex nitrile dimers, and in particular adenine, should be addressed in detail with new detections of HNCHCN in more interstellar sources and with chemical modelling.

ACKNOWLEDGEMENTS

We thank the anonymous referee for his/her instructive comments and suggestions. V.M.R. has received funding from the European Union's H2020 research and innovation programme under the Marie Skłodowska-Curie grant agreement No 664931. J.M.-P. acknowledges partial support by the MINECO and FEDER funding under grants ESP2015-65597-C4-1 and ESP2017-86582-C4-1-R.

REFERENCES

- Agúndez M., et al., 2015, *Astronomy and Astrophysics*, **579**, L10
 Armijos-Abendaño J., Martín-Pintado J., Requena-Torres M. A., Martín S., Rodríguez-Franco A., 2014, *Monthly Notices of the Royal Astronomical Society*, **446**, 3842
 Balucani N., 2009, *International Journal of Molecular Sciences*, **10**, 2304
 Balucani N., 2012, *Chemical Society Reviews*, **41**, 5473
 Bernstein M. P., Ashbourn S. F. M., Sandford S. A., Allamandola L. J., 2004, *The Astrophysical Journal*, **601**, 365
 Chakrabarti S., Chakrabarti S. K., 2000, *Astronomy and Astrophysics*, **354**, L6
 Clemmons J. H., Jasien P. G., Dykstra C. E., 1983, *Molecular Physics*, **48**, 631
 Ehrenfreund P., Glavin D. P., Botta O., Cooper G., Bada J. L., 2001, *Proceedings of the National Academy of Sciences*, **98**, 2138
 Endres C. P., Schlemmer S., Schilke P., Stutzki J., Mäijller H. S. P., 2016, *Journal of Molecular Spectroscopy*, **327**, 95
 Eschenmoser A., 2007, *Tetrahedron*, **63**, 12821
 Ginsburg A., et al., 2016, *Astronomy & Astrophysics*, **586**, A50
 Guesten R., Walmsley C. M., Ungerechts H., Churchwell E., 1985, *Astronomy and Astrophysics*, **142**, 381

- Hasegawa T., Sato F., Whiteoak J. B., Miyawaki R., 1994, [The Astrophysical Journal Letters](#), 429, L77
- Henshaw J. D., Longmore S. N., Kruijssen J. M. D., 2016, [Monthly Notices of the Royal Astronomical Society: Letters](#), 463, L122
- Hüttemeister S., Wilson T. L., Bania T. M., Martín-Pintado J., 1993, *Astronomy and Astrophysics*, 280, 255
- Jung S. H., Choe J. C., 2013, [Astrobiology](#), 13, 465
- Kaiser R. I., Balucani N., 2001, [Accounts of Chemical Research](#), 34, 699
- Krieger N., et al., 2017, [The Astrophysical Journal](#), 850, 77
- Martín S., Requena-Torres M. A., Martín-Pintado J., Mauersberger R., 2008, [The Astrophysical Journal](#), 678, 245
- McElroy D., Walsh C., Markwick A. J., Cordiner M. A., Smith K., Millar T. J., 2013, [Astronomy and Astrophysics](#), 550, A36
- Melosso M., et al., 2018, [Astronomy and Astrophysics](#), 609, A121
- Müller H. S. P., Thorwirth S., Roth D. A., Winnewisser G., 2001, [Astronomy and Astrophysics](#), 370, L49
- Müller H. S. P., Schlöder F., Stutzki J., Winnewisser G., 2005, [Journal of Molecular Structure](#), 742, 215
- Oró J., 1961, [Nature](#), 191, 1193
- Pickett H. M., Poynter R. L., Cohen E. A., Delitsky M. L., Pearson J. C., Müller H. S. P., 1998, [Journal of Quantitative Spectroscopy and Radiative Transfer](#), 60, 883
- Puzzarini C., 2015, [The Journal of Physical Chemistry A](#), 119, 11614
- Requena-Torres M. A., Martín-Pintado J., Rodríguez-Franco A., Martín S., Rodríguez-Fernández N. J., de Vicente P., 2006, [Astronomy & Astrophysics](#), 455, 971
- Requena-Torres M. A., Martín-Pintado J., Martín S., Morris M. R., 2008, [The Astrophysical Journal](#), 672, 352
- Rivilla V. M., Fontani F., Beltrán M. T., Vasyunin A., Caselli P., Martín-Pintado J., Cesaroni R., 2016, [The Astrophysical Journal](#), 826, 161
- Rivilla V. M., Beltrán M. T., Cesaroni R., Fontani F., Codella C., Zhang Q., 2017a, [Astronomy and Astrophysics](#), 598, A59
- Rivilla V. M., Beltrán M. T., Martín-Pintado J., Fontani F., Caselli P., Cesaroni R., 2017b, [Astronomy and Astrophysics](#), 599, A26
- Rivilla V. M., et al., 2018, [Monthly Notices of the Royal Astronomical Society](#),
- Rodríguez-Fernández N. J., Martín-Pintado J., de Vicente P., Fuente A., Hüttemeister S., Wilson T. L., Kunze D., 2000, *Astronomy and Astrophysics*, 356, 695
- Rodríguez-Fernández N. J., Martín-Pintado J., Fuente A., de Vicente P., Wilson T. L., Hüttemeister S., 2001, [Astronomy and Astrophysics](#), 365, 174
- Rodríguez-Fernández N. J., Martín-Pintado J., Fuente A., Wilson T. L., 2004, [Astronomy and Astrophysics](#), 427, 217
- Shivani Misra A., Tandon P., 2017, [Research in Astronomy and Astrophysics](#), 17, 1
- Smith I. W. M., Talbi D., Herbst E., 2001, [Astronomy and Astrophysics](#), 369, 611
- Takano S., Sugie M., Sugawara K.-i., Takeo H., Matsumura C., Masuda A., Kuchitsu K., 1990, [Journal of Molecular Spectroscopy](#), 141, 13
- Tercero B., Kleiner I., Cernicharo J., Nguyen H. V. L., López A., Muñoz Caro G. M., 2013, [The Astrophysical Journal Letters](#), 770, L13
- Vazart F., Latouche C., Skouteris D., Balucani N., Barone V., 2015, [The Astrophysical Journal](#), 810, 111
- Wakelam V., et al., 2012, [The Astrophysical Journal Supplement](#), 199, 21
- Yim M. K., Choe J. C., 2012, [Chemical Physics Letters](#), 538, 24
- Zaleski D. P., et al., 2013, [The Astrophysical Journal Letters](#), 765, L10
- Zeng S., et al., 2018, [Monthly Notices of the Royal Astronomical Society](#),

478, 2962

APPENDIX A: SPECTRA OF ^{13}CN AND NCCNH^+

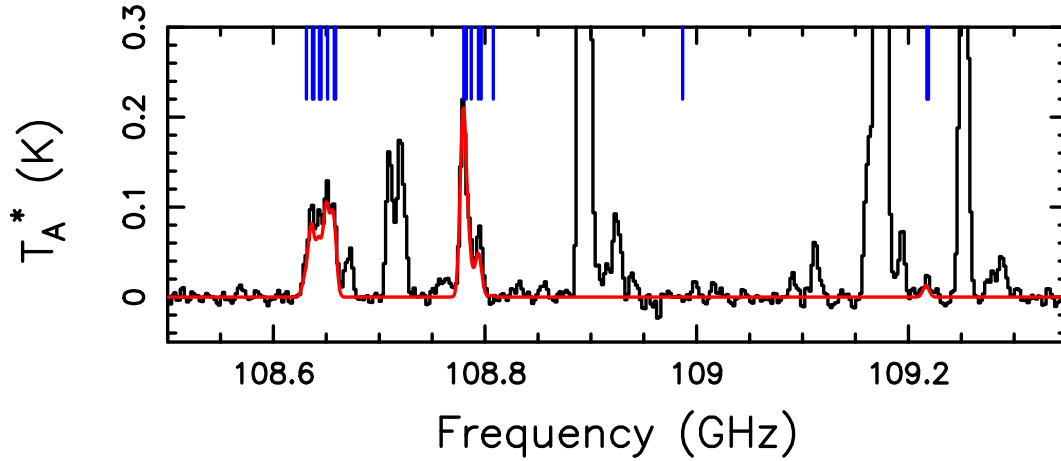
This paper has been typeset from a $\text{T}_{\text{E}}\text{X}/\text{L}^{\text{A}}\text{T}_{\text{E}}\text{X}$ file prepared by the author.

Table A1. Spectroscopic information from CDMS molecular database of the transitions of ^{13}CN detected towards G+0.693.

Frequency (GHz)	Transition	$\log A_{ul}$ (s^{-1})	E_{up} (K)
108.631121	1 1 1 0 – 0 1 0 1	-5.0188	5.2
108.636923	1 1 1 1 – 0 1 0 1	-5.0172	5.2
108.638212	1 2 1 1 – 0 1 1 0	-5.4444	5.2
108.643590	1 2 1 2 – 0 1 1 1	-5.5926	5.2
108.644346	1 2 1 0 – 0 1 1 1	-5.0188	5.2
108.645064	1 2 1 1 – 0 1 1 1	-5.5620	5.2
108.651297	1 1 1 2 – 0 1 0 1	-5.0095	5.2
108.657646	1 2 1 2 – 0 1 1 2	-5.1411	5.2
108.658948	1 2 1 1 – 0 1 1 2	-5.4775	5.2
108.780010	1 2 2 3 – 0 1 1 2	-4.9788	5.2
108.782374	1 2 2 2 – 0 1 1 1	-5.1107	5.2
108.786982	1 2 2 1 – 0 1 1 0	-5.2430	5.2
108.793753	1 2 2 1 – 0 1 1 1	-5.3502	5.2
108.796400	1 2 2 2 – 0 1 1 2	-5.5604	5.2
108.807788	1 2 2 1 – 0 1 1 2	-6.4897	5.2
108.986836	1 1 0 1 – 0 1 0 1	-7.2578	5.2
109.217567	1 2 1 2 – 0 1 0 1	-6.1603	5.2
109.218323	1 2 1 0 – 0 1 0 1	-6.0475	5.2
109.218919	1 2 1 1 – 0 1 0 1	-6.0932	5.2

Table A2. Spectroscopic information from CDMS molecular database of the transitions of NCCNH^+

Frequency (GHz)	Transition	$\log A_{ul}$ (s^{-1})	E_{up} (K)
detected towards G+0.693.			
88.758103	10–9	-3.7928	23
97.633424	11–10	-3.6668	28

**Figure A1.** IRAM 30m spectra of ^{13}CN towards the Galactic Center quiescent giant molecular cloud G+0.693. The red curves correspond to the LTE best fit obtained with MADCUBA–AUTOFIT. The vertical blue lines indicate the position of the transitions presented in Table A1.

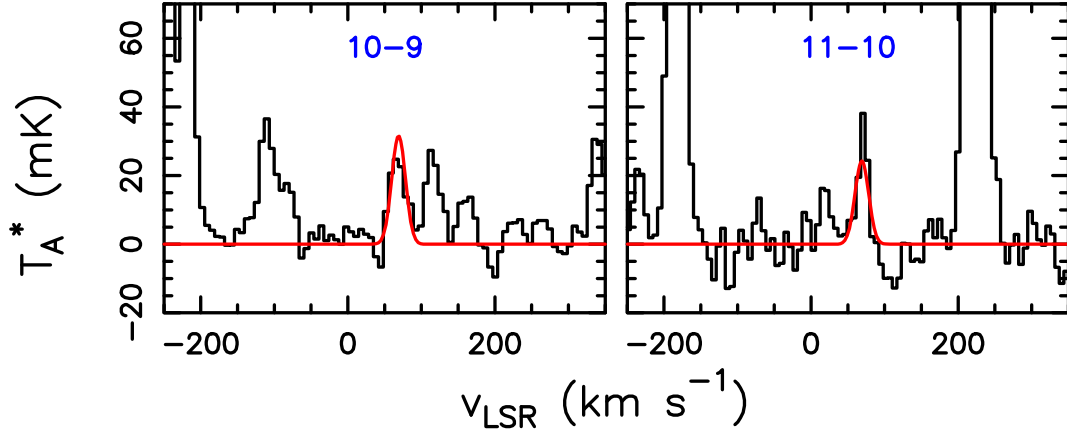


Figure A2. IRAM 30m spectra of NCCNH^+ towards the Galactic Center quiescent giant molecular cloud G+0.693. The red curves correspond to the LTE best fit obtained with MADCUBA-AUTOFIT.